3D fracture behaviour of graphite specimens weakened by V- notches with end holes under mixed mode (I+II) loading

H. Salavati[1*], H. Mohammadi[2], Y. Alizadeh[3], M.R. Ayatollahi[4]

[1]Department of Mechanical Engineering, Shahid Bahonar University of Kerman, Kerman, Iran

[2]Laboratori de Càlcul Numèric (LaCàN), Universitat Politècnica de Catalunya (UPC), Barcelona, Spain

[3]Department of Mechanical Engineering, Amirkabir University of Technology, Tehran, Iran

[4] Center of Excellence in Experimental Solid Mechanics and Dynamics, School of Mechanical Engineering, Iran University of Science and Technology, Tehran, Iran

ABSTRACT

In the present contribution, the static strength of isostatic graphite using V-notched specimens with end holes under mixed mode loading is investigated considering 3D simulation. An experimental program was performed and in total, 14 new experimental data are provided in the paper for the first time. The criterion based on the averaged value of the strain energy density over a control volume which has been applied to assess the static strength of the different 2D specimens, is developed in the current work by modification of the control volume to assess the thickness effect on the static strength of graphite specimens. A sound agreement is found between the experimental data and the results obtained from the strain energy density criterion.

Keywords: Brittle failure, Thickness, V- notch with end hole, Mixed mode, Graphite

[*]Corresponding Author: Hadi Salavati
Email: hadi_salavati@uk.ac.ir
Tel: +98 34 32111763
Fax: +98 34 32120964

1. Introduction

Isostatic graphite is formed by means of Cold Isostatic Pressing (CIP) technique and is characterized by its homogeneous structure and excellent isotropic electrical, thermal and mechanical properties. Sometimes it is purified in special-designed graphitization furnace to remove non-carbonaceous impurities. It is widely used in various industrial and scientific engineering as a structural and/or functional material. In most of industrial products of graphite such as moulds, heating elements, chucks, screws, rolls, etc. some notches of U or V-shapes are viewed as desirable entities under different loadings. The notches are weak points that may generate cracks and lead to brittle fracture. Extensive studies on brittle fracture of cracked graphite specimens are present in literature. For example, the mixed mode (I+II) fracture behavior of two polycrystalline graphite was studied by Awaji and Sato [1] who used the Brazilian Disk (BD) specimen. Some other researchers used the single-edge notch bending specimen [2] and the three-point bending sandwiched specimen [3] to study the fracture testing on graphite.

Burchell [4] proposed a theory by relating brittle fracture of graphite to the crack nucleation and the subcritical crack growth from pre-existing pores under the influence of the stress field associated with the pores or defects. Lomakin et al. [5] used the energy release rate criterion to find the fracture characteristics of graphite materials under plane strain conditions. Becker et al. [6] used the Digital Image Correlation (DIC) technique and the finite element method to calculate the J-integral for two different specimen geometries (four point bend and a double torsion) of nuclear grade coarse polygranular graphite. The theory of Maximum Tangential Stress (MTS) originally proposed by Erdogan and Sih [7], was modified by Ayatollahi and Aliha [8] to estimate mixed mode fracture in two grades of polycrystalline graphite containing sharp cracks. Other works related to the fracture behaviour of cracked components made of graphite or graphite composites are well highlighted in Refs. [9-11]. Dealing with notch problems, there are very few papers have dealt with brittle fracture in sharp and rounded tip notched graphite components.

Probably, Bazaj and Cox [12] made the first work to study the brittle fracture of notched graphite components. In their work, the stress-concentration and fatigue-strength-reduction factors were determined for grooved tensile specimens made of a fine-grained graphite (Great Lakes Carbon grade H205). Kawakami [13] tested three different kinds of graphite including IG-11 (fine grained isotropic graphite), Stackpole 2020 (SP2020, fine grained isotropic graphite) and PGX (moulded anisotropic graphite) and studied the notch sensitivity on the material behaviour.

Ayatollahi and Torabi [14] conducted a series of fracture tests on three different rounded-tip V-notched specimens made of a polycrystalline graphite material. Moreover, the RV-MTS (Rounded tip V-notch MTS) theory was used to determine the notch fracture toughness. The successful application of RV-MTS criterion for other materials can be found in other works by the same authors [15-18]. In another work [19], the fracture load and the fracture initiation angle were experimentally measured for a V-notched specimen made of a polycrystalline graphite under combined tensile-shear loading. Then, the RV-MTS theory was used to estimate the experimental values of the notch fracture resistance and the fracture initiation angle for the tested graphite specimens.

A recent approach, based on the Strain Energy Density (SED), was proposed and successfully applied for the fracture assessment of notched components. The SED approach is based on the evaluation of the averaged strain energy density over a control volume. The criterion was applied to assess the fracture behaviour of different materials under mode I, mixed mode and torsion loading [20-23]. As shown well in Refs. [24,25], the criterion can be applied to assess the fatigue strength of welded joints and notched components. Recently, the SED criterion has been applied to study the static strength of functionally graded materials under mode I [26,27] and mixed mode loading [28-30]. Recently, the SED approach was used to investigate the fracture behavior of Tungsten- Cooper functionally graded material which has been produced by powder metallurgy technique for the first time [31-34]. The SED approach was used to investigate the static strength of sharp and rounded-tip V-notched components made of polycrystalline graphite subjected to different degrees of loading mixity, ranging from pure mode I to pure mode II [35]. In that work, a good set of experimental data were provided

by using Brazilian disk specimens. Berto et al. [36] studied the brittle fracture of isostatic polycrystalline graphite experimentally, theoretically and numerically using U-notched samples under mode I and mixed mode loading (I+II) considering different combinations of the notch radius and the tilt angle of the notch. Brittle fracture of polycrystalline graphite under torsion loading was studied experimentally and theoretically using axisymmetric specimens weakened by sharp and rounded-tip V-notches [37]. In that paper, a new set of experimental data was provided from notched samples made of isostatic polycrystalline graphite with different values of notch opening angle and root radius, which should be useful to engineers engaged with static strength analysis of graphite components. Moreover, the SED approach was applied to the torsion loading of notched graphite specimens. Dealing with the key-hole notches, Lazzarin et al. [38] investigated the fracture behaviour of specimens made of isostatic graphite and weakened by inclined key-hole notches. Finally, the SED criterion was used to summarise all the data in a single scatter band independent of the notch geometry and mode mixity.

In the present contribution, brittle fracture in isostatic graphite is studied experimentally and numerically using VO-notched samples under mixed mode loading (I+II) considering different values of thickness. An experimental programme was performed to provide a new set of results for the first time. In total 14 new data are provided in the paper. Moreover, a modified SED criterion is proposed to assess the critical fracture load of the specimens with different values of thickness. In this study, only one notch geometry (notch opening angle, notch depth and notch tip radius) and one mode mixity is considered. It is worthwhile mentioning that the proposed criterion can be applied to various notch geometries and mode mixities.

2. Material Properties

The fracture tests were performed on a commercial isostatic graphite. The main mechanical properties of the tested graphite are summarized in the table. 1. The Young's modulus was obtained by using load-displacement curve of a tensile test performed of a plate specimen. To measure tensile strength

(σ_t) bending tests were performed on specimens weakened by single U-notch with a radius of 10 mm and a depth of 20 mm.

The thickness, width, and length of the specimens was 20, 40, and 200 mm. In order to determine the value of σ_t and K_{Ic} two experiments were performed on specimens and the average value was used for theoretical predictions. The discrepancies between maximum and minimum values of σ_t and K_{Ic} were about 3% and 1%, respectively.

3. Experimental procedure

The VO- notched beam specimens were produced to perform experimental tests. The geometry of the specimens is shown in Fig. 1. A constant width and length of 40 and 200 mm, respectively were considered for the specimens and different thicknesses of 10-15-20-25-30-35-40 mm were produced. For all specimens, a constant geometry of VO-notch was considered as shown in Fig. 1. Two specimens were produced for each thickness providing 14 VO- notched beam specimens as shown in Fig. 2. All the specimens were accurately fabricated by using CNC water-jet machine. Before conducting the experiments, the cut surfaces of the graphite specimens were polished by using a fine abrasive paper to remove any possible local stress concentrations due to surface roughness. In order to obtain mixed mode I+II loading condition, the load was applied at a distance 30 mm from the notch bisector line. The horizontal distances of supports from the center of the specimen were considered to be 80 mm and 30 mm. The experiments were performed by a ZWICK 1494 testing device under displacement control with a constant displacement rate of 0.2 mm/min. A VO- notched beam specimen under three-point bending test is shown in Fig. 3. Fig. 4 shows a sample load–displacement curve for the case t = 25mm. Moreover, Fig. 5 shows a broken specimen within the test machine.

4. The modified averaged strain energy density criterion to assess the thickness effect on fracture

The averaged SED criterion states that brittle fracture occurs when the averaged value of the SED over a well-defined control volume is equal to a critical value W_c [2]. W_c is a material-dependent

value which is independent of notch geometry. For brittle materials, W_c can be evaluated as follow [2]:

$$W_c = \frac{\sigma_t^2}{2E} \tag{1}$$

where σ_t is the maximum normal stress existing at the edge of the notch at the moment of initiation of fracture.

In plane problems, the control volume becomes a circle or a circular sector with a radius R_c in the case of cracks or pointed V-notches in mode I or mixed, I + II, mode loading. A useful expression for the radius R_c surrounding the control volume has been provided for the crack case under plane strain condition.

$$R_{c_{P.Stn}} = \frac{(1 + v)(5 - 8v)}{4\pi} \left(\frac{K_{Ic}}{\sigma_t}\right)^2 \tag{2}$$

where K_{Ic} is the fracture toughness and v is the Poisson's ratio.

In the case of VO-notches, the area assumes a crescent shape, with R_c being its maximum width as measured along the notch bisector line. Under mixed-mode loading, the control area is no longer centred with respect to the notch bisector, but rigidly rotated with respect to it and centred on the point where the SED (and the maximum principal stress) reaches its maximum value. The outer radius of the control area is equal to $R_c + r_0$ as shown in Fig. 6. The value of r_0 can be determined as follow [6]:

$$r_0 = \frac{q - 1}{q}\rho$$

$$q = \frac{2\pi - 2\alpha}{\pi} \tag{3}$$

Nevertheless, the mentioned criterion is not able to predict the thickness effects. In this case, in order to predict the thickness effect on the fracture loads of specimens, the averaged SED criterion is modified. This criterion covers the thicknesses which are in the range of plane strain condition.

6

For all thicknesses, the control volume is redefined assuming a constant volume of material surrounding the notch tip to be the determinant factor of fracture. This constant volume assumed to be equal to the control volume of a cracked specimen with a thickness of $t_{P.Stn}$. In Single edge bending (SE(B)) and compact tension (C(T)) specimens, $t_{P.Stn}$ is equal to W/2, where W is the width of the specimen.

In addition, the whole thickness of the specimens is involved to the initiation of fracture. Therefore, the greater the thickness of the specimen, the smaller the cross section area of the control volume. So, the relation between control radius and thickness is as follow:

$$A.t = \pi.R^2_{c_{P.Stn}}.t_{P.Stn}$$

$$A = \pi(r_0 + R_c)^2 - [(r_0 + R_c)^2 \cos^{-1}\frac{(\rho-r_0)^2+(r_0+R_c)^2-\rho^2}{2(\rho-r_0)(r_0+R_c)} + \tag{4}$$

$$\rho^2 \cos^{-1}\frac{(\rho-r_0)^2-(r_0+R_c)^2+\rho^2}{2\rho(\rho-r_0)} - \frac{1}{2}\sqrt{R_c(2r_0 + R_c)(2\rho + R_c)(2\rho - 2r_0 - R_c)}]$$

where, A is the cross section area of the control volume, t is the thickness of the specimen, R_c is the control radius of a 3D specimen and ρ is the notch tip radius. Fig. 7 illustrates the mentioned definition of the control volume schematically.

It should be noted that this modified criterion can be applied to different notch geometries and mode mixities. For each geometry of the notch and each mode mixity, first the control volume of the reference cracked specimen (Fig. 7) should be determined by using the original averaged SED as described earlier in the paper. Then, by means of the modification presented in this study, the control volume of different thicknesses can be determined.

5. SED approach in analysis of the thickness effect on fracture of the VO-notched graphite specimens

In order to obtain the crack initiation point and the averaged value of SED over the control volume, some finite element analyses were carried out by using ABAQUS software version 6.11. It was assumed that the crack initiation angle do not depend on the thickness while it depends on notch

geometry and mode mixity. So, in order to find the crack initiation point, a finite element analysis was performed under plane strain condition and linear elastic hypothesis. The point on the edge of the notch on which the principal stress is maximum was considered the point of the initiation of the fracture. Then, for each thickness, 3D finite element analysis was carried out defining the control volume as described in the previous section. 20-node quadratic brick elements as shown in Fig. 8 were used in the 3D models. Fig. 9 shows the maximum principal stress and SED contour lines for the configuration t=40mm. Table 2 summarizes the theoretical and experimental results of fracture loads. A good agreement between experimental fracture loads and theoretical predictions can be observed. Fig. 10 plot the experimental results and the theoretical predictions of the ratio of critical fracture load to thickness as a function of the thickness. In this figure, the results of theoretical predictions based on two methods have been summarized. In the first method, the cross section of the control volume was considered to be constant for all the thicknesses and it was determined based on the original ASED for plane-strain condition. Besides, the thickness of the control volume was considered to be equal to the thickness of the specimen. In the second method, the results were obtained based on the modified ASED. As the figure shows, the modified ASED can describe the effect of thickness on fracture behaviour of VO-notched graphite specimens with a better accuracy.

6. Conclusion

In the present work, the average value of strain energy density (SED) over a modified control volume ahead of the notch tip was used to obtain the critical fracture load of VO- notched specimens made of isostatic graphite under mixed mode loading.

The main findings of the present work can be summarized as follows:

1. The average deviation between the theoretical and the experimental values in terms of the critical fracture loads was found to be limited (3.6%).

2. The mean value of SED over the modified control volume suggested in the present paper can be used to consider 3D effects on the fracture bahaviour of graphite specimens.

7. References

1. H. Awaji, S. Sato, Combined Mode Fracture Toughness Measurement by the Disk Test, *Journal of Engineering Materials and Technology*, 100(2), 175-182 (1978)
2. N.M. Yamauchi Y., Kishida K., Okabe T., Measurement of Mixed-Mode Fracture Toughness for Brittle Materials Using Edge-Notched Half-Disk Specimen, *Journal of the Society of Materials Science, Japan*, 50(3), 229-234 (2001)
3. M. Li, M. Tsujimura, M. Sakai, Crack-face grain interlocking/bridging of a polycrystalline graphite: The role in mixed mode fracture, *Carbon*, 37(10), 1633-1639 (1999)
4. T.D. Burchell, A microstructurally based fracture model for polygranular graphites, *Carbon*, 34(3), 297-316 (1996)
5. E.V. Lomakin, A.I. Zobnin, A.V. Berezin, Finding the fracture toughness characteristics of graphite materials in plane strain, *Strength Mater*, 7(4), 484-487 (1975) (in English)
6. T.H. Becker, M. Mostafavi, R.B. Tait, T.J. Marrow, An approach to calculate the J-integral by digital image correlation displacement field measurement, *Fatigue & Fracture of Engineering Materials & Structures*, 35(10), 971-984 (2012)
7. F. Erdogan, Sih G. C, On the crack extension in plates under plane loading and transverse shear, *ASME Journal of Basic Engineering*, 58(4), 519-527 (1963)
8. M.R. Ayatollahi, M.R.M. Aliha, Mixed mode fracture analysis of polycrystalline graphite – A modified MTS criterion, *Carbon*, 46(10), 1302-1308 (2008)
9. M. Mostafavi, T.J. Marrow, Quantitative in situ study of short crack propagation in polygranular graphite by digital image correlation, *Fatigue & Fracture of Engineering Materials & Structures*, 35(8), 695-707 (2012)
10. S. Sato, H. Awaji, H. Akuzawa, Fracture toughness of reactor graphite at high temperature, *Carbon*, 16(2), 95-102 (1978)
11. L. Shi, H. Li, Z. Zou, A.S.L. Fok, B.J. Marsden, A. Hodgkins, P.M. Mummery, J. Marrow, Analysis of crack propagation in nuclear graphite using three-point bending of sandwiched specimens, *Journal of Nuclear Materials*, 372(2–3), 141-151 (2008)
12. D.K. Bazaj, E.E. Cox, Stress-concentration factors and notch-sensitivity of graphite, *Carbon*, 7(6), 689-697 (1969)
13. K. H., Notch sensitivity of graphite materials for VHTR, *J Atomic Energy Soc Jpn*, 27(4), 357-364 (1985)
14. M.R. Ayatollahi, A.R. Torabi, Failure assessment of notched polycrystalline graphite under tensile-shear loading, *Materials Science and Engineering: A*, 528(18), 5685-5695 (2011)
15. M.R. Ayatollahi, A.R. Torabi, A criterion for brittle fracture in U-notched components under mixed mode loading, *Engineering Fracture Mechanics*, 76(12), 1883-1896 (2009)
16. M.R. Ayatollahi, A.R. Torabi, Determination of mode II fracture toughness for U-shaped notches using Brazilian disc specimen, *International Journal of Solids and Structures*, 47(3–4), 454-465 (2010)
17. M.R. Ayatollahi, A.R. Torabi, Experimental verification of RV-MTS model for fracture in soda-lime glass weakened by a V-notch, *J Mech Sci Technol*, 25(10), 2529-2534 (2011) (in English)
18. M.R. Ayatollahi, A.R. Torabi, P. Azizi, Experimental and Theoretical Assessment of Brittle Fracture in Engineering Components Containing a Sharp V-Notch, *Exp Mech*, 51(6), 919-932 (2011) (in English)

19. M.R. Ayatollahi, A.R. Torabi, Tensile fracture in notched polycrystalline graphite specimens, *Carbon*, 48(8), 2255-2265 (2010)

20. F. Berto, E. Barati, Fracture assessment of U-notches under three point bending by means of local energy density, *Materials & Design*, 32(2), 822-830 (2011)

21. F. Berto, D.A. Cendon, P. Lazzarin, M. Elices, Fracture behaviour of notched round bars made of PMMA subjected to torsion at −60 °C, *Engineering Fracture Mechanics*, 102(0), 271-287 (2013)

22. F. Berto, M. Elices, P. Lazzarin, M. Zappalorto, Fracture behaviour of notched round bars made of PMMA subjected to torsion at room temperature, *Engineering Fracture Mechanics*, 90(0), 143-160 (2012)

23. P. Lazzarin, A. Campagnolo, F. Berto, A comparison among some recent energy- and stress-based criteria for the fracture assessment of sharp V-notched components under Mode I loading, *Theoretical and Applied Fracture Mechanics*, 71(0), 21-30 (2014)

24. P. Lazzarin, F. Berto, D. Radaj, Fatigue-relevant stress field parameters of welded lap joints: pointed slit tip compared with keyhole notch, *Fatigue & Fracture of Engineering Materials & Structures*, 32(9), 713-735 (2009)

25. D. Radaj, F. Berto, P. Lazzarin, Local fatigue strength parameters for welded joints based on strain energy density with inclusion of small-size notches, *Engineering Fracture Mechanics*, 76(8), 1109-1130 (2009)

26. E. Barati, Y. Alizadeh, A numerical method for evaluation of J-integral in plates made of functionally graded materials with sharp and blunt V-notches, *Fatigue & Fracture of Engineering Materials & Structures*, 34(12), 1041-1052 (2011)

27. E. Barati, Y. Alizadeh, J.A. Mohandesi, J-integral evaluation of austenitic–martensitic functionally graded steel in plates weakened by U-notches, *Engineering Fracture Mechanics*, 77(16), 3341-3358 (2010)

28. H. Salavati, Y. Alizadeh, F. Berto, Effect of notch depth and radius on the critical fracture load of bainitic functionally graded steels under mixed mode I + II loading, *Phys Mesomech*, 17(3), 178-189 (2014) (in English)

29. A.Y. Salavati H., Kazemi A., Berto F. , A new expression to evaluate the critical fracture load for bainitic functionally graded steels under mixed mode (I+II) loading *Engineering Failure Analysis*, 5(3), 12-15 (2014)

30. H. Salavati, Y. Alizadeh, F. Berto, Fracture Assessment of Notched Bainitic Functionally Graded Steels under Mixed Mode (I + II) Loading, *Phys Mesomech*, 18(4), 307-325 (2015)

31. H. Mohammadi, H. Salavati, Y. Alizadeh, F. Berto, Prevalent mode II fracture assessment of inclined U-notched specimens made of tungsten-copper functionally graded material, *Theoretical and Applied Fracture Mechanics*, 89, 90-99 (2017)

32. H. Mohammadi, H. Salavati, Y. Alizadeh, F. Berto, S.V. Panin, Fracture investigation of V-notch made of tungsten-copper functionally graded materials, *Phys Mesomech*, 20(4), 457-464 (2017)

33. H. Mohammadi, H. Salavati, M.R. Mosaddeghi, A. Yusefi, F. Berto, Local strain energy density to predict mixed mode I+II fracture in specimens made of functionally graded materials weakened by V-notches with end holes, *Theoretical and Applied Fracture Mechanics*, 92, 47-58 (2017)

34. H. Salavati, H. Mohammadi, A. Yusefi, F. Berto, Fracture assessment of V-notched specimens with end holes made of tungsten-copper functionally graded material under mode I loading, *Theoretical and Applied Fracture Mechanics*, (2017)

35. M.R. Ayatollahi, F. Berto, P. Lazzarin, Mixed mode brittle fracture of sharp and blunt V-notches in polycrystalline graphite, *Carbon*, 49(7), 2465-2474 (2011)

36. F. Berto, P. Lazzarin, C. Marangon, Brittle fracture of U-notched graphite plates under mixed mode loading, *Materials & Design*, 41(0), 421-432 (2012)

37. F. Berto, P. Lazzarin, M.R. Ayatollahi, Brittle fracture of sharp and blunt V-notches in isostatic graphite under torsion loading, *Carbon*, 50(5), 1942-1952 (2012)
38. P. Lazzarin, F. Berto, M.R. Ayatollahi, Brittle failure of inclined key-hole notches in isostatic graphite under in-plane mixed mode loading, *Fatigue & Fracture of Engineering Materials & Structures*, 36(9), 942-955 (2013)

Figures

Figure 1. The geometry of the specimens (Dimensions are in mm)

Figure 2. Views of some different V-notched specimens with end-hole with different thickness

Figure 3. The graphite specimens within the test machine under mixed mode loading.

Figure 4. A sample load-displacement curve for the case t=25mm

Figure 5. A broken specimen within the test machine

Figure 6. Control volume in VO- notched specimens a) mode I b) mixed mode

Figure 7. Definition of the control volume schematically for considertion the thickness effect

Figure 8. 20-node quadratic brick elements in 3D models

Figure 9. Maximum principal stress and strain energy density contour lines for the case t=40mm

Figure 10. Experimental and theoretical ratio of critical fractures load to thickness versus the thickness

Figure 1
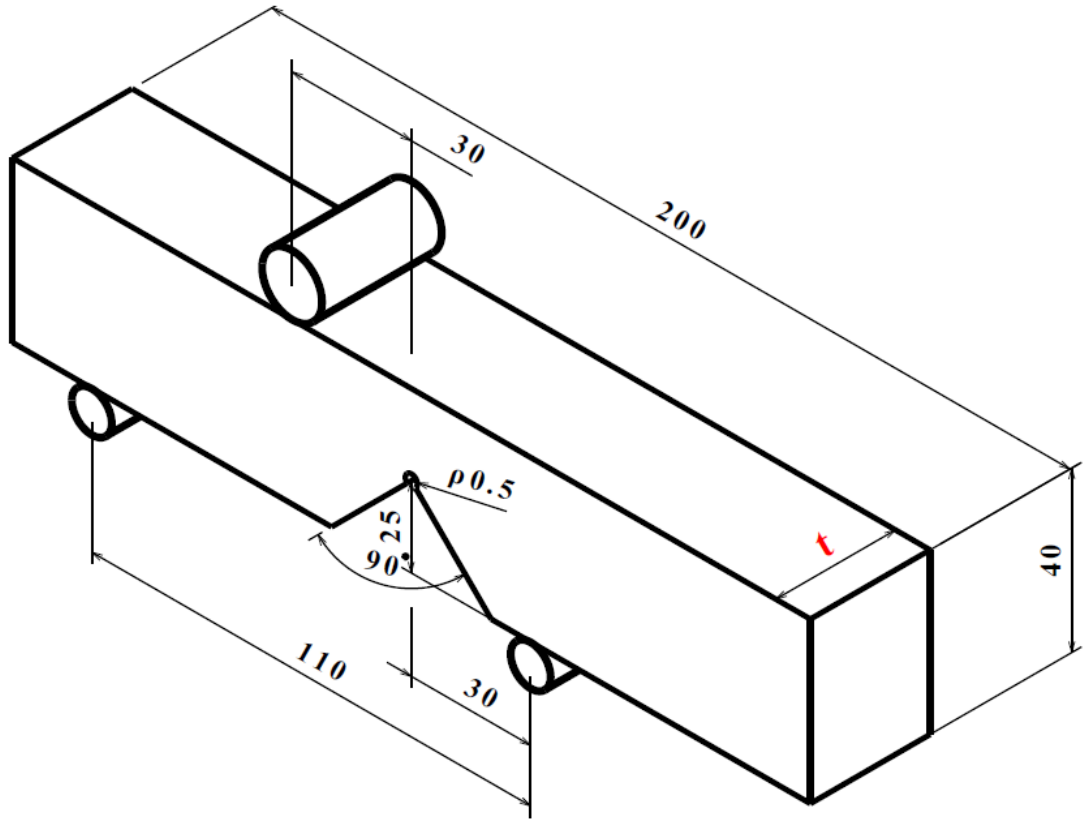
Figure. 2

Figure. 3

Figure. 4

Figure. 6

Figure. 7

$$V_{P.Stn} = \pi . R_{c_{P.Stn}}^2 . t_{P.Stn}$$

$R_{c_{P.Stn}}$

Control Volume of the reference cracked specimen

$$\boldsymbol{V_1} = \boldsymbol{V_2} = \boldsymbol{V_{P.Stn}}$$
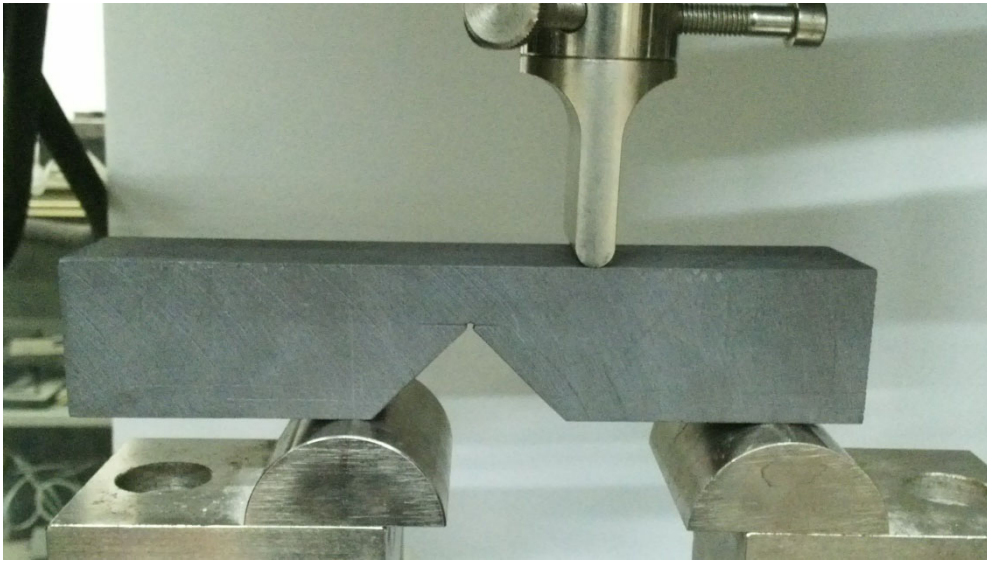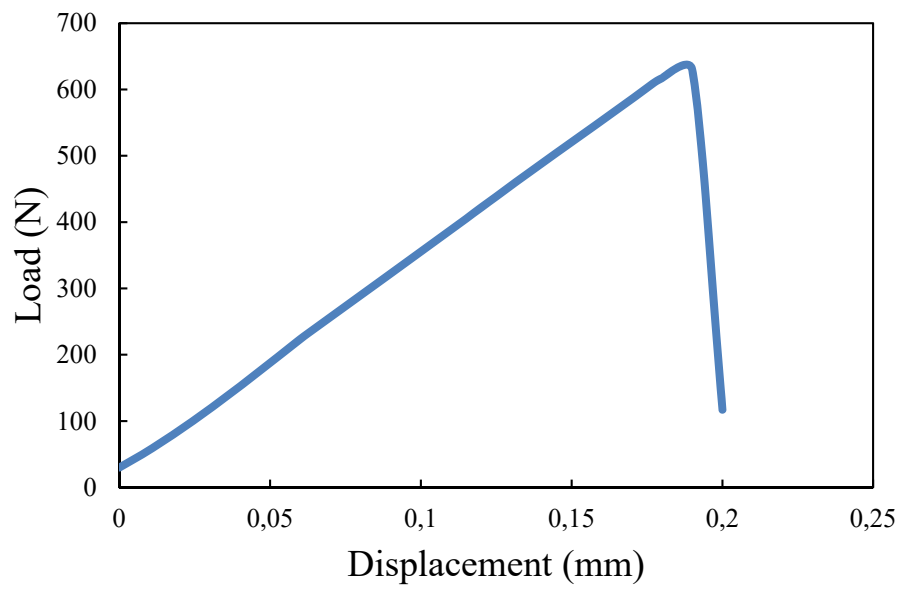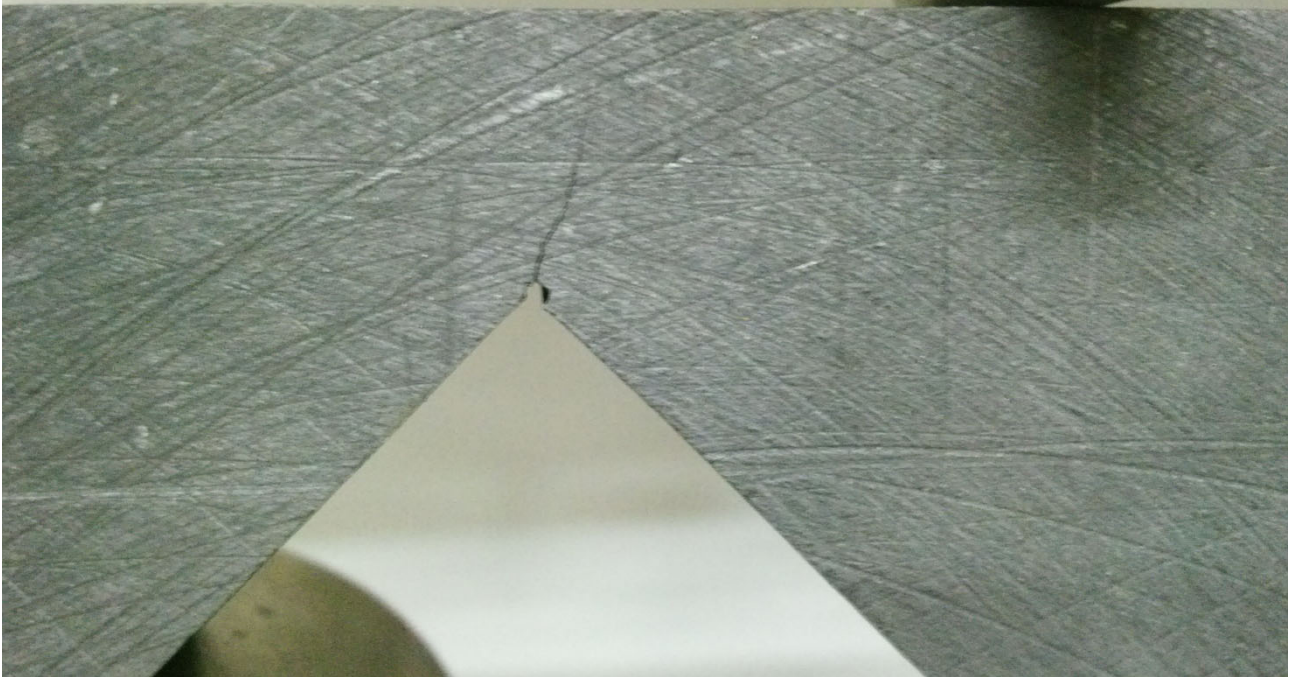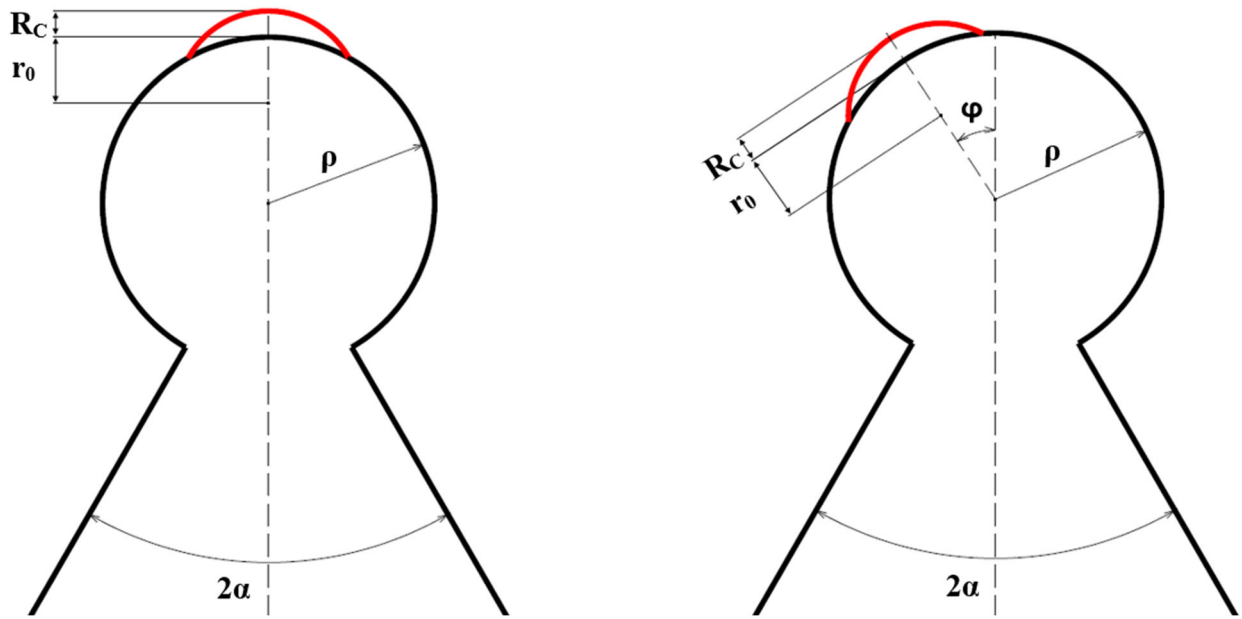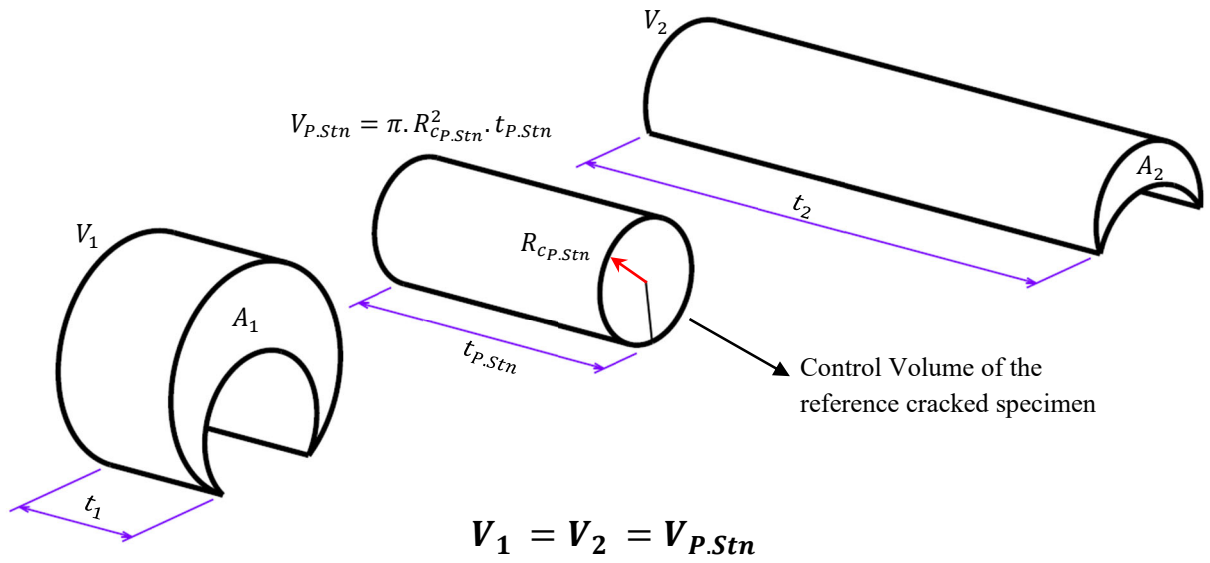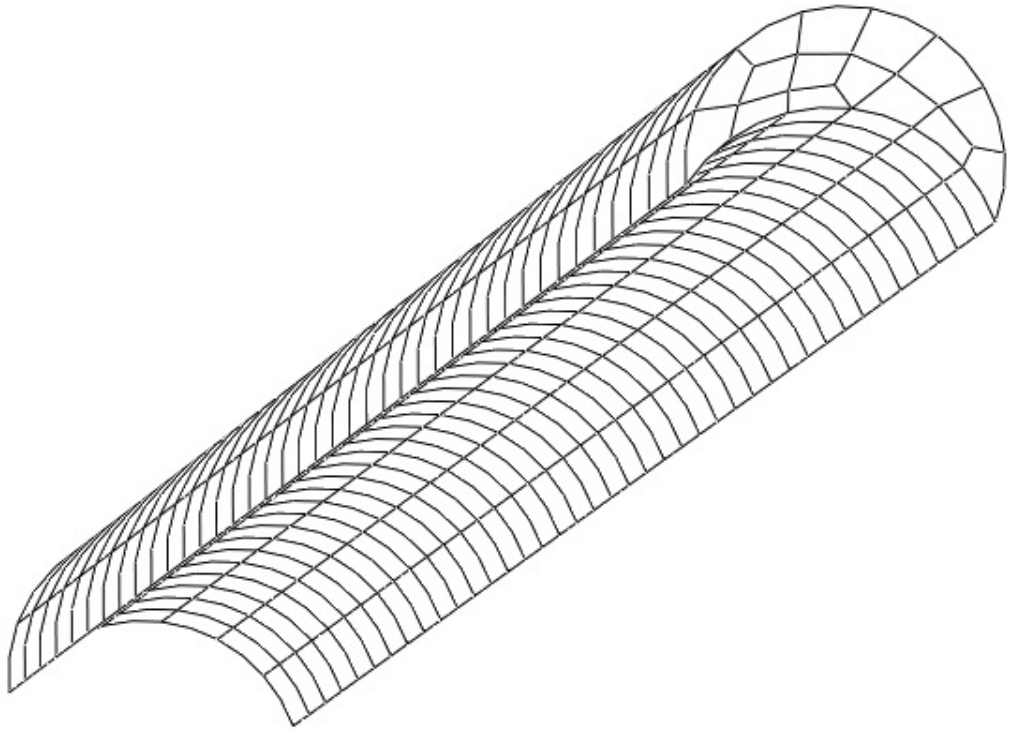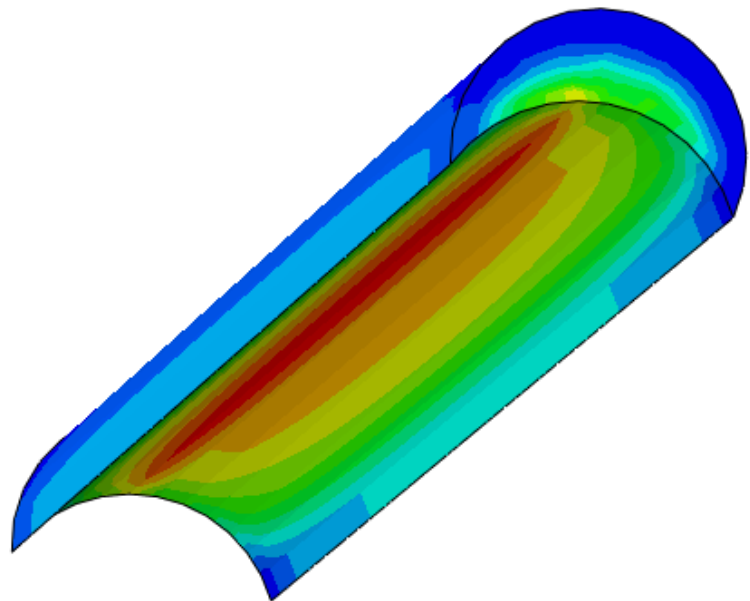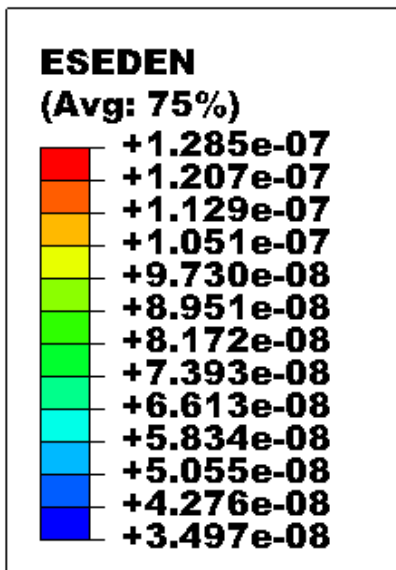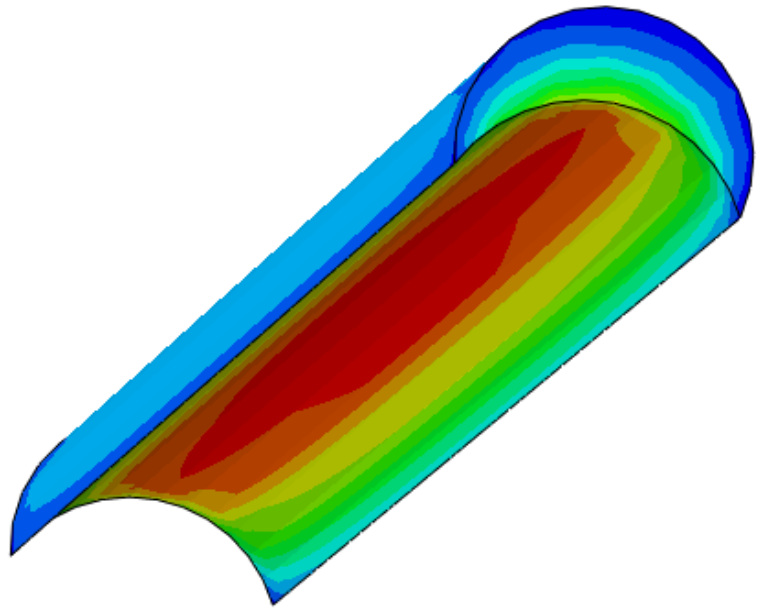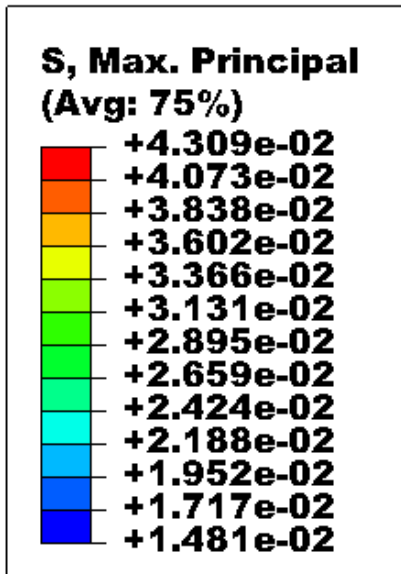
Figure. 8

Figure. 9

Figure. 10
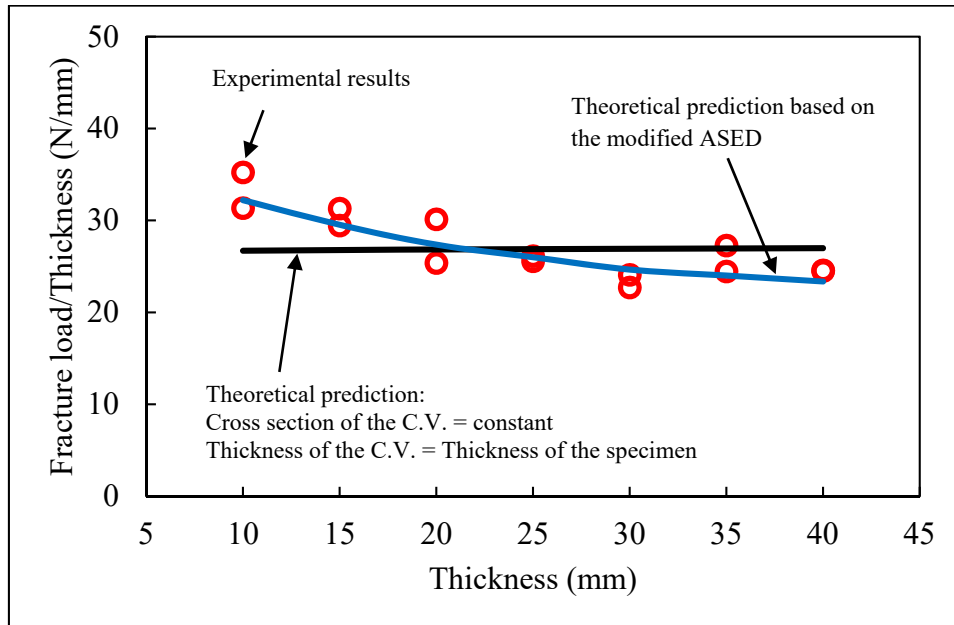
Table 1. Mechanical properties of the tested isostatic graphite

Material property	Value
Elasticity modulus E(Gpa)	5.2 ± 0.5
Poisson's ratio ν	0.2
Plane strain fracture toughness K_{Ic}(MPa.m$^{0.5}$)	0.84
σ_t (MPa)	23.74

Table 2. Comparison of the experimental results (F_{Exp}) with theoretical predictions (F_{th})

Thickness	R_c (mm)	SED (J/m^3)	F_{Th}	F_{Th}/Thickness (N/mm)	F_{Exp} (N)	F_{Exp}/F_{Th}
10	0.59	5.22E-07	322.10	32.21	313.45	0.97
					352.36	1.09
15	0.49	2.76E-07	443.07	29.54	441.83	1.00
					469.40	1.06
20	0.42	1.81E-07	547.37	27.37	602.69	1.10
					507.40	0.93
25	0.38	1.28E-07	650.19	26.01	639.15	0.98
					653.24	1.00
30	0.34	9.90E-08	739.96	24.67	681.43	0.92
					722.49	0.98
35	0.32	7.67E-08	840.49	24.01	855.47	1.02
					954.74	1.14
40	0.3	6.20E-08	934.54	23.36	982.93	1.05
					979.87	1.05